

Effects of Cavitation from Extracorporeal Shock Wave Combined with Sulfur Hexafluoride Microbubble on Myocardial Ultrastructure in Rats

ABSTRACT

Background: In the present study, the effects of extracorporeal cardiac shock waves combined with different concentrations of sulfur hexafluoride ultrasound microbubbles on myocardial ultrastructure in rats were observed.

Methods: Thirty-six rats were randomly divided into 6 groups: control group (N), extracorporeal cardiac shock wave group, and combined group, i.e., extracorporeal cardiac shock wave combined with different concentrations of sulfur hexafluoride microbubble (0.225 mL/kg/min, 0.45 mL/kg/min, 0.9 mL/kg/min, 1.8 mL/kg/min). The combination of extracorporeal cardiac shock wave combined with sulfur hexafluoride microbubbles of different concentrations had no significant effect on hemodynamic indexes and left ventricular function in rats.

Results: There were significant differences in cardiac troponin I (cTnI) and nitric oxide among different groups. Histopathology showed that inflammatory cells infiltrated in the shock wave + microbubble 0.9 and shock wave + microbubble 1.8 groups. The myocardial ultrastructural injury score of shock wave + microbubble 1.8 group was significantly higher than that of the N group, shock wave group, shock wave + microbubble 0.225 group, and shock wave + microbubble 0.45 group. The score of shock wave + microbubble 0.9 group was higher than that of the control group ($P = .009$). Western blot results showed that the expression of vascular endothelial growth factor and endothelial nitric oxide synthase (eNOS) protein in the rats treated with extracorporeal cardiac shock wave combined with sulfur hexafluoride microbubbles of different concentrations was higher than that in the N group and shock wave group, with shock wave + microbubble 0.45 group having the strongest expression.

Conclusion: Myocardial ultrastructure damage occurs when high concentrations of sulfur hexafluoride microbubbles are present, but a proper concentration of sulfur hexafluoride microbubbles could promote the cavitation effect of extracorporeal cardiac shock waves. Thus combination therapy may become a new paradigm in coronary heart disease, especially contributing to the treatment of refractory angina. Combination therapy may change coronary heart disease treatment, especially for refractory angina.

Keywords: Extracorporeal cardiac shock wave, sulfur hexafluoride, ultrasonic microbubble, cavitation effect, shearing stress, transmission electron microscope, myocardial ultrastructure

INTRODUCTION

At present, the prevalence and mortality of cardiovascular diseases are still on the rise. According to the data from China's Cardiovascular Health and Disease Report 2020, the number of people suffering from cardiovascular diseases has reached 330 million, and the death from cardiovascular diseases is the primary cause of death for urban and rural residents.¹ Coronary heart disease (CHD) is the most common type of cardiovascular disease, which is very easy to cause acute myocardial infarction and can threaten the life of patients in severe cases. In recent years, a variety of treatment methods, such as percutaneous coronary intervention, coronary artery bypass grafting, and thrombolytic drugs, have saved more and more lives of patients with acute myocardial infarction, but there are still some patients who turn into refractory angina.² Currently, treatment for

ORIGINAL INVESTIGATION

Yajing Miao¹ 

Xiaoxu Wang¹ 

Hongning Yin¹ 

Ruoling Han² 

¹Department of Echocardiography, the Second Hospital of Hebei Medical University, Shijiazhuang, Hebei, China

²Department of Ultrasound, The Fourth Hospital of Hebei Medical University, Shijiazhuang, Hebei, China

Corresponding author:

Ruoling Han
✉ hr1_63523@sina.com

Received: January 5, 2023

Accepted: April 19, 2023

Available Online Date: May 22, 2023

Cite this article as: Miao Y, Wang X, Yin H, Han R. Effects of cavitation from extracorporeal shock wave combined with sulfur hexafluoride microbubble on myocardial ultrastructure in rats. *Anatol J Cardiol.* 2023;27(9):519-528.



Copyright©Author(s) - Available online at anatoljcardiol.com.
Content of this journal is licensed under a Creative Commons Attribution-NonCommercial 4.0 International License.

DOI:10.14744/AnatolJCardiol.2023.2946

patients with advanced CHD includes revascularization of chronic occlusion, external counterpulsation, myocardial laser revascularization, and stem cell therapy, but the effect is not satisfactory.³

Extracorporeal cardiac shock wave (SW) is a therapy developed in recent years to treat severe CHD. Its mechanism is to apply physical principles to stimulate the local ischemic myocardium with low energy, so as to produce mechanical shear stress and cavitation effect in the cells of myocardial tissue, increase the concentration of nitric oxide (NO) and vascular endothelial growth factor (VEGF) in the local myocardium, and promote angiogenesis and collateral circulation in the treatment area, thereby improving the myocardial blood supply, relieving angina symptoms, and reducing the occurrence of ischemic events.⁴ It has been proved that SW can improve myocardial perfusion in patients with chronic intractable angina and enhance left ventricular systolic function and exercise tolerance.^{5,6} In animal experiments, SW has been proven to reduce myocardial cell apoptosis, regulate autophagy, and inhibit myocardial fibrosis after acute myocardial infarction in rats.⁷⁻⁹ In 2022, China formulated an expert consensus on extracorporeal SW therapy for CHD, which provides a new treatment option for patients with refractory CHD in the late stage.¹⁰

Sulfur hexafluoride (SonoVue) microbubbles (MBs) can enter the left heart cavity and myocardial microcirculation through the pulmonary circulation after peripheral intravenous injection and have been widely used in cardiac ultrasound examination of patients with CHD. The MB will produce shear stress and cavitation effect after blasting and release a lot of energy which can collapse the microcirculation thrombus and increase the myocardial microcirculation blood flow perfusion.¹¹ In addition, after the MB explosion, eNOS pathway is activated, which increases endothelial nitric oxide (NO) synthase concentration by 6 times and blood perfusion rate by 2.5 times.¹²

Both extracorporeal cardiac SWs and sulfur hexafluoride MBs can affect the myocardium by the mechanism of cavitation effect and shearing stress. In our previous results from in vitro experiment, we confirmed that extracorporeal SW can destroy MBs, which is more significant than that under ultrasonic blasting. However, whether the mechanical shearing stress and cavitation effect generated by extracorporeal cardiac SW combined with sulfur hexafluoride

MBs during treatment will lead to additional tissue damage remains to be verified. The ultrasonic MB is concentration dependent, with the higher MB concentration having more significant effect.¹³ In previous studies, 0.9 mL/kg/min sulfur hexafluoride MBs were injected. All rats successfully obtained high-quality real-time MCE short-axis images at the level of middle papillary muscle, with MBs evenly filling in the myocardium.¹⁴ Therefore, we propose and identify a novel hypothesis: a proper concentration of sulfur hexafluoride MBs could promote the cavitation effect of extracorporeal cardiac SWs. It may provide theoretical support for the treatment of patients with CHD, especially contributing to the treatment of refractory angina.

In this study, a rat model was adopted to observe the effects of extracorporeal cardiac SW combined with different concentrations of sulfur hexafluoride MBs on myocardial structure, including its macroscopic, functional, and ultrastructure. Different MB concentrations were set accordingly to observe whether the damage was related to the concentration of sulfur hexafluoride MBs. Specifically, echocardiography, serum cTnI level and NO concentration, western blot of eNOS and VEGF, hematoxylin and eosin (H&E) and Masson staining, and transmission electron microscopy (TEM) to evaluate the possible damage of extracorporeal SW combined with sulfur hexafluoride MBs on myocardial ultrastructure.

METHODS

Animals

Thirty-six 8-week-old male Sprague Dawley (SD) rats [without specific pathogen (SPF) grade], weighing 180-200 g, were provided by Hebei Ex & In Vivo Biotechnology Co., Ltd. (Shijiazhuang, China, Certificate No.: SCXK [Ji] 2020-002). Sprague Dawley rats were randomly divided into 6 groups (n=6): group 1: normal control group (N group); group 2: extracorporeal cardiac SW group; group 3: extracorporeal cardiac SW combined with the concentration 0.225 mL/kg/min cardiac SW combined with the concentration 0.45 mL/kg/min of ultrasonic MB (SW + MB0.45); group 5: extracorporeal of ultrasonic MB (SW + MB0.225); group 4: extracorporeal cardiac SW combined with the concentration 0.9 mL/kg/min of ultrasonic MB (SW + MB0.9); and group 6: extracorporeal cardiac SW combined with the concentration 1.8 mL/kg/min of ultrasonic MB (SW + MB1.8).

Anesthesia

RWD small animal anesthesia machine (Shenzhen, China, model R500) was used. The induction concentration of isoflurane was adjusted to 3%-4%, and the concentration was maintained at 2%-2.5%. The animals were kept in complete anesthesia during the operation.

Preparation and Infusion Method of Sulfur Hexafluoride Microbubbles

In order to ensure that the injection volume of each rat is equal, we configure 2 concentrations of sulfur hexafluoride MBs. In the first method, 59 mg sulfur hexafluoride MBs (SonoVue, Bracco, Italy) was mixed with 5 mL of normal saline and shaken rapidly for 20 seconds to form 5 mL of uniform

HIGHLIGHTS

- To assist advanced coronary heart disease therapy, sulfur hexafluoride microbubble concentrations were varied to see whether they affected damage.
- The ideal concentration of sulfur hexafluoride microbubbles does not affect the myocardial ultrastructure in rats, whereas 1.8 mL/kg/min does.
- Sulfur hexafluoride microbubbles may also boost extracorporeal cardiac shock wave cavitation.

suspension, with the average diameter of ultrasonic MB of 2.5 μm and an concentration of $2 \times 10^8/\text{mL}$. In the second method, 59 mg sulfur hexafluoride MBs (SonoVue, Bracco, Italy) was mixed with 2.5 mL of normal saline and shaken rapidly for 20 seconds to form 5 mL of uniform suspension, with the average diameter of ultrasonic MB of 2.5 μm and an concentration of $4 \times 10^8/\text{mL}$.

Each rat was weighed before infusion, and sulfur hexafluoride MB suspension was extracted according to body weight. In order to ensure that the volume of injection fluid of each rat was equal, the corresponding suspension was extracted with 1 mL syringe and normal saline was added to 1 mL. For the group of SW + MB0.225, SW + MB0.45, and SW + MB0.9, the first method of suspension was used for the rat. For the group of SW + MB1.8, the second method of suspension was used for the rat. For the group of Normal and SW, saline infusion was used for the rat. In the group of extracorporeal SWs combined with ultrasound MBs of different concentrations, sulfur hexafluoride MBs were infused at a uniform rate through the tail vein 15 seconds during the SW treatment until the end of the SW treatment.

Treatment

On the first, third, and fifth days after randomization, rats were treated with extracorporeal cardiac SW therapeutic apparatus (Storz Medical, Switzerland) and ALOKA

ultrasonic system (HITACHI, Japan), probe model (9133, 20 Hz) (Figure 1). The extracorporeal cardiac SW combined with ultrasound MBs of different concentrations were used for treatment. The anesthetized rats were fixed in the supine position on the operating table, and the SW probe was closely contacted with the chest skin. After connecting a 1 mL syringe through the rat tail vein puncture, the rats received extracorporeal cardiac SW therapy (energy: 0.1 mJ/mm; frequency: 1.0 Hz; the number of SWs: 200 times). Waiting 15 seconds before SW treatment, different concentrations of sulfur hexafluoride MBs (0.225 mL/kg/min, 0.45 mL/kg/min, 0.9 mL/kg/min, 1.8 mL/kg/min) were infused. The same amount of normal saline was injected into the tail vein of rats in SW group at the same time of SW treatment. Place the SW probe in front of the chest of rats in group N without the SW therapy. Rats in group N received the same amount of normal saline through the tail vein of rats. Echocardiography was used to monitor heart rate and rhythm during treatment. Blood pressure was measured with the tail artery blood pressure analysis system (Softron BP-2010) before and after the third treatment.

Echocardiography

A GE vivid E95 color Doppler ultrasonic diagnostic instrument equipped with 12-s high-frequency probe (frequency 12 MHz) and Echo PAC workstation is used. M-mode

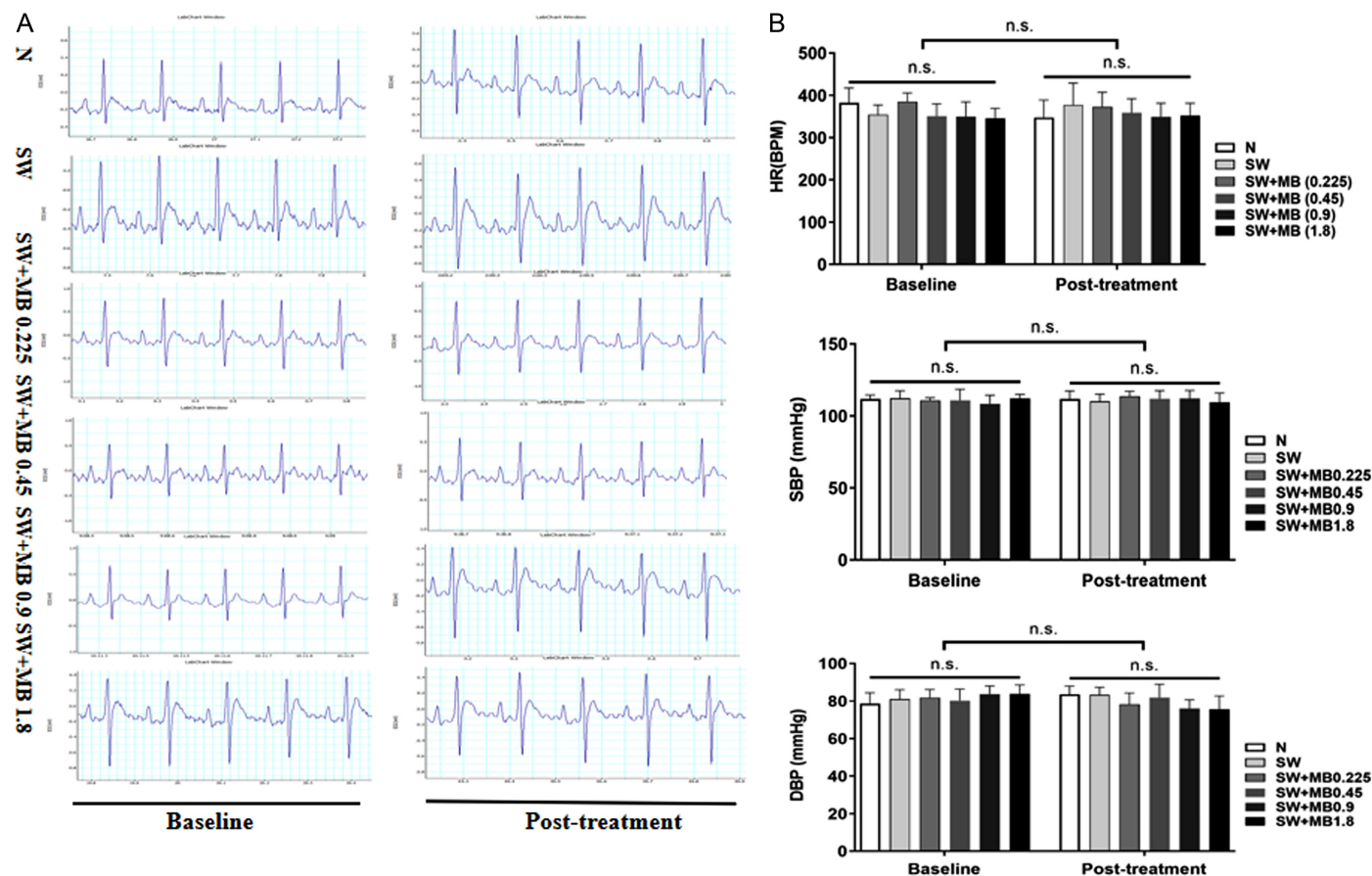


Figure 1. (A) ECG monitoring before and during treatment in each group showed no malignant arrhythmia and ST-T abnormality. (B) There was no significant difference in heart among groups before and after treatment ($P > .05$). n.s, not significant.

echocardiography images were acquired on the short axis cardiac at the papillary muscle level of the left ventricle and the images were stored digitally for offline analysis. The measurement of the left ventricular short-axis papillary muscle section end-diastolic diameter (LVEDD) and end-systolic diameter (LVESD) was repeated and the left ventricular short-axis shortening rate (FS) and ejection fraction (LVEF) was calculated. The average value was used for statistical analysis.

Determination of Serum cTnI level and Nitric Oxide Concentration

Before treatment and after the end of the third treatment, 0.5 mL of blood was taken from the rat jugular vein and left for half an hour. The blood was centrifuged for 10 minutes at a speed of 3000 rpm and take out the supernatant. The cTnI level in rat plasma was determined with a highly sensitive ELISA kit (cloud clone core, SEA478Ra, USA). The concentration of NO was determined with the NO determination kit (microplate method; Nanjing, China, A013-2-1).

Myocardial Tissue Collection

Myocardial tissues were collected from all rats on the eighth day after treatment. Rats were anesthetized by intraperitoneal injection of 7% chloral hydrate solution with a dose of 0.5 mL per 100 g. The rats were placed on the hypothermic operating platform after the reflex disappeared to make the heart stop at the end of diastole. Immediately open the chest through the sternal angle approach, clip, and cut off the large blood vessels at the bottom of the heart to take off the heart. Divide the heart into 4 segments along the long axis of the left ventricle, and cut the heart one by one along the cross-section. The first apical segment was discarded and the second segment was fixed in a 4% paraformaldehyde solution and was embedded in paraffin for histopathological examination. The third segment (papillary muscle level) was treated according to the following procedure of electron microscope sample collection. The remaining myocardial tissue obtained from electron microscopy was placed in a 4 mL centrifuge tube and frozen in a refrigerator at -80°C for subsequent extraction of myocardial protein.

Hematoxylin and Eosin Staining

A paraffin section of myocardial tissue (thickness: 5 μm) was prepared and it was stained with H&E. Three high-magnification visual fields were randomly selected for each slice, and histopathological observation was conducted with an optical microscope (Lm, BX51, Olympus, Japan). Observe the distribution of neutrophils and lymphocytes in myocardial tissue by evaluating the degree of inflammation.

Masson Staining

The paraffin section of myocardial tissue (thickness of 5 μm) for Masson staining was prepared. Histopathological observation was carried out under an optical microscope (Lm, BX51, Olympus), and the degree of myocardial fibrosis was evaluated in 3 microscopic fields (200 \times) of every 5 μm left ventricular myocardial slice.

Assessment of Myocardial Ultrastructural Damage

The rat myocardial tissue was cut into small pieces of 1 \times 1 mm and then immersed completely into 2.5% glutaraldehyde and stored at 4°C for more than 2 hours for anterior fixation. About 0.1 mol/L phosphate buffer (pH 7.4) was used to wash the tissues for 3 hours, and then the tissues were immersed in 1% osmic acid for 1 hour for fixation, followed by rinsing with 0.1 mol/L phosphate buffer for 15 minutes. The tissue was immersed with 50%, 70%, 80%, and 95% acetone successively for 15 minutes each time, and then it was immersed with 100% acetone twice for 20 minutes each time to complete the tissue dehydration. The tissue was put into EPON 812 solution (acetone : resin=1 : 2) at room temperature overnight. The treated tissue was put into the embedding plate with resin. The embedded plate was placed into the temperature box as the temperature changed to 37°C for 12 hours, 45°C for 12 hours, and 60°C for 48 hours successively. The wrapped tissue block was cut into ultrathin sections with a thickness of about 50 nm by an ultrathin microtome. The section was incubated with uranium dioxide acetate for 30 minutes and lead citrate for 30 minutes for electronic staining. All sections were observed with an electron microscope and photographed with a digital imaging system.

For the acquired 36 electron microscopic specimens, 10 visual fields were randomly selected from each specimen. An electron microscope was used to score the myocardial ultrastructure injury, and the difference was compared between the 2 groups. According to Yildirim et al.¹⁵ myocardial ultrastructure damage was evaluated.

Western Blot

Western blot was used to analyze the effects of different intervention methods on eNOS and VEGF in all groups. The enhanced chemiluminescence reagent is used to detect the imaging of protein. β -actin was used as an internal control to standardize the expression of eNOS and VEGF.

Statistical Analysis

Statistical analysis Statistical Package for the Social Sciences (SPSS) 23.0 was used for statistical analysis. The data are expressed as mean \pm SD. Two-way ANOVA was used to analyze the differences between baseline and post-treatment and among multiple groups. Kruskal–Wallis test is used for grade data. $P < .05$ was considered statistically significant. GraphPad Prism 8.0 (San Diego, Calif, USA) was used to generate statistical charts. The related indexes of heart size and systolic function (including LVEDD, LVESD, LVEF, FS) and TnI, NO were analyzed by 2-way ANOVA. The myocardial ultrastructure score belongs to the grade data and is tested by Kruskal–Wallis test (the figure is not shown).

RESULTS

Changes of Heart Rhythm, Heart Rate, and Blood Pressure

In order to evaluate the effect of extracorporeal SW combined with MBs of different concentrations on the hemodynamics of rats, we recorded the electrocardiogram of rats, and no arrhythmia occurred in all rats (Figure 1A). The heart rate and blood pressure of rats were measured at baseline

and after treatment. The results showed that there was no significant difference in heart rate, systolic blood pressure, and diastolic blood pressure among the baseline groups ($P > .05$). After treatment, there was no statistical difference in heart rate, systolic blood pressure, and diastolic blood pressure compared with the baseline ($P > .05$), and there was no statistical difference in heart rate, systolic blood pressure, and diastolic blood pressure among the groups after treatment ($P > .05$) (Figure 1B).

Effects of Extracorporeal Shock Wave Combined with Microbubbles on Left Ventricular Morphology

To further evaluate the effect of extracorporeal cardiac SW combined with different concentrations of MBs on the cardiac function of rats, cardiac ultrasound was used to observe the size and systolic function of the left ventricle of rats at baseline and after treatment. The results showed that LVEDD (cm), LVESD (cm), LVEF%, and FS% of rat hearts in each group had no significant difference at baseline and after treatment ($P > .05$) (Figure 2A-D).

Changes of cTnI and Nitric Oxide in Serum

In order to evaluate whether there is myocardial injury after extracorporeal SW combined with MBs of different concentrations, the level of cTnI in the rat blood samples was measured. The results showed that cTnI had significant differences among different groups and before and after treatment ($P < .001$), with significant interaction ($P < .001$). There was no significant difference among the groups before treatment ($P >$

.05). After treatment, the cTnI levels in SW + MB0.9 group and SW + MB1.8 group were significantly higher than that in the N group, SW group, SW + MB0.225 group, and SW + MB0.45 group ($P < .05$). There was no significant difference among the rest groups. The results of the comparison among groups before and after treatment showed that the cTnI levels in SW + MB0.9 group and SW + MB1.8 group after treatment were significantly higher ($P < .001$) (Figure 3A).

To evaluate whether extracorporeal SW combined with MBs of different concentrations can promote the production of NO, we detected the level of NO in rat serum. The results showed that there were significant differences in NO among different groups and between before and after treatment ($P < .05$), and the interaction was significant ($P < .05$). There was no significant difference among the groups before treatment ($P > .05$). After treatment, the NO levels in SW group, SW + MB0.225 group, SW + MB0.45 group, SW + MB0.9 group, and SW + MB1.8 group were higher than that in N group, and the NO level in SW + MB1.8 group was higher than that in SW group. There was no significant difference among the rest groups. After treatment, the level of NO in SW group, SW + MB0.225 group, SW + MB0.45 group, SW + MB0.9 group, and SW + MB1.8 group increased significantly (Figure 3B).

Pathological Changes of Myocardium

Histopathology method was used to evaluate the effect of extracorporeal SW combined with MB therapy on myocardial tissue. Myocardial tissue sections of rats were observed

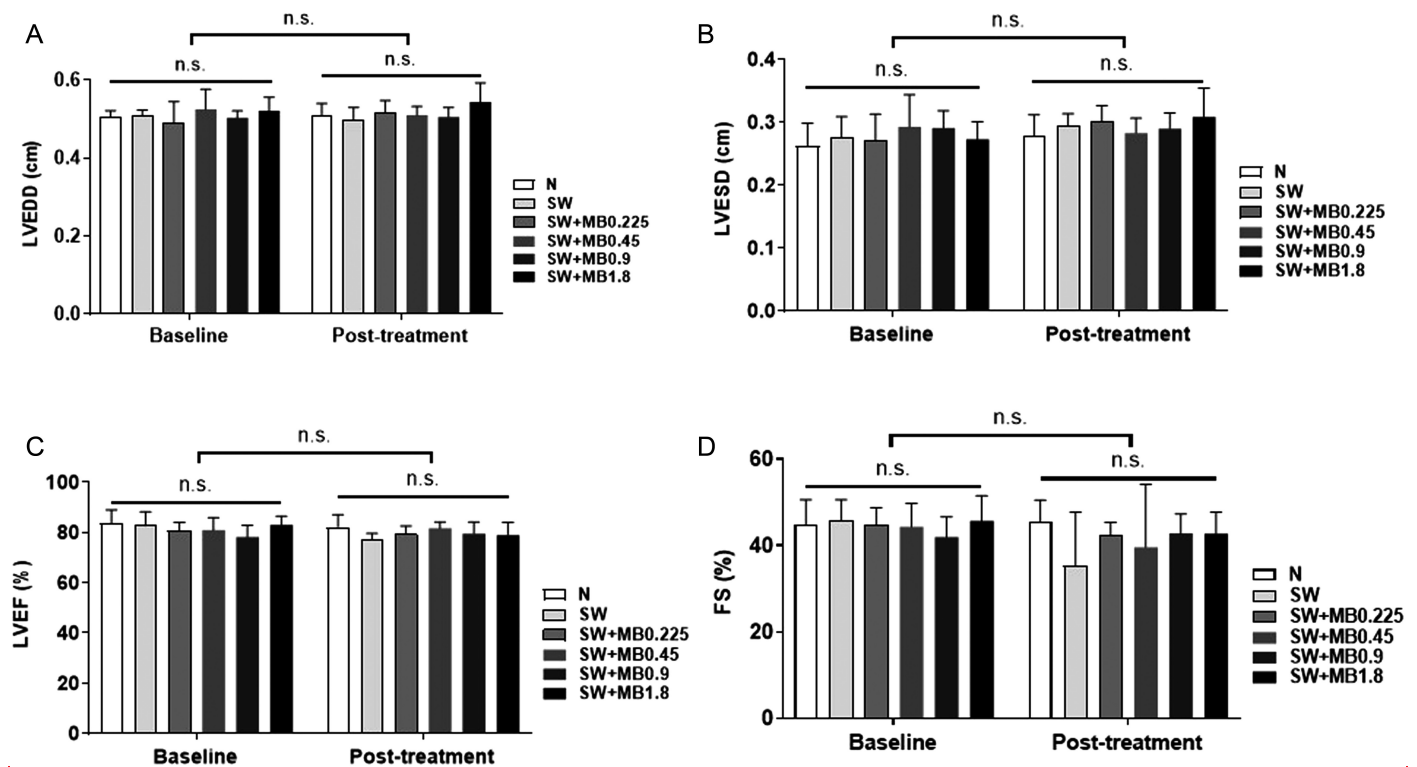


Figure 2. A, B, C, and D respectively showed the changes of LVEDD (cm), LVESD (cm), LVEF%, and FS% before and after treatment. The results showed that there was no statistical difference before and after treatment ($P > .05$), and there was no statistical difference among the groups after treatment ($P > .05$). FS, short-axis shortening rate; LVEDD, left ventricular end-diastolic diameter; LVEF, left ventricular ejection fraction; LVESD, left ventricular end-systolic diameter; n.s., not significant.

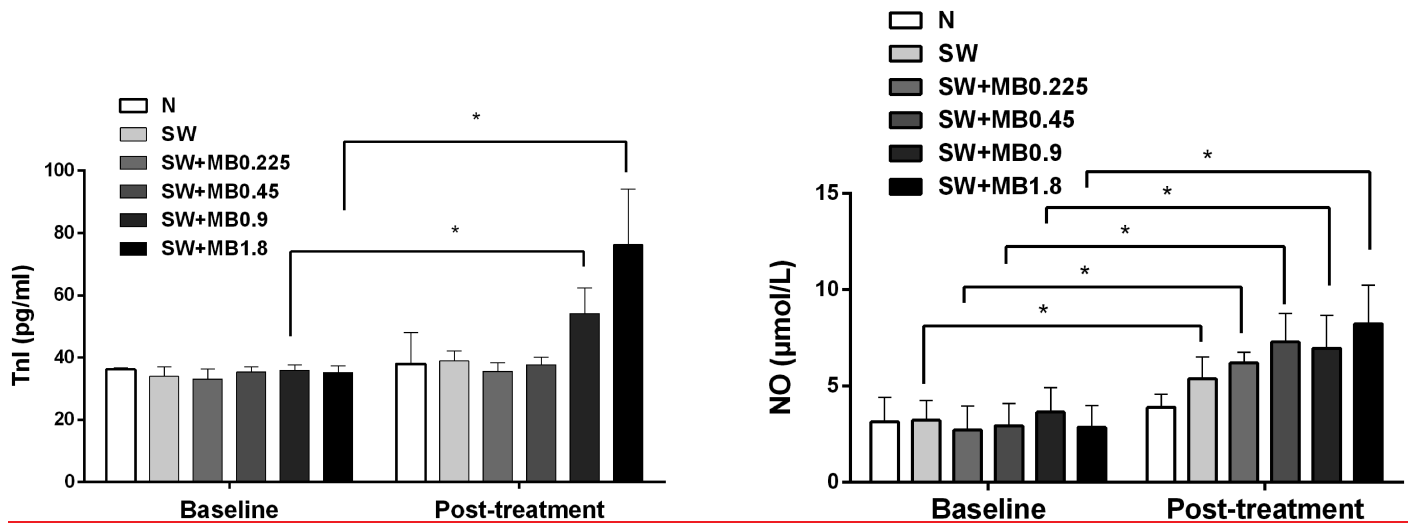


Figure 3. (A) There are significant differences among different groups and between before and after treatment in the level of cTnl ($P < .001$). **(B)** There are significant differences among different groups and between before and after treatment in the level of nitric oxide ($P < .001$)

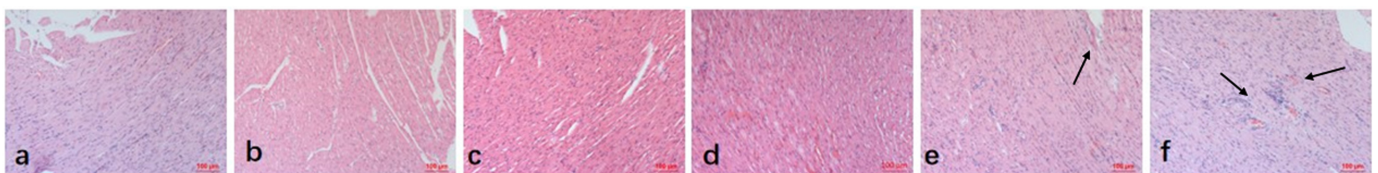
under a light microscope after H&E and Masson staining. Inflammatory cell infiltration was found in SW + MB0.9 group and SW + MB1.8 group, and no abnormality was found in other groups (Figure 4A). An increase in the degree of fibrosis was also found in SW + MB1.8 group, while the degree of myocardial fibrosis in other groups was not significant (Figure 4B).

Ultrastructural Changes of Rat Myocardium

In order to further determine the effect of extracorporeal SW combined with ultrasound MB therapy on myocardial ultrastructure, the structure of myocardial collagen fibers, important organelles, nuclei, mitochondria, and sarcoplasmic reticulum in rats were observed by TEM. The results showed that there was no collagenous fiber proliferation

in N group and SW group, slight collagenous fiber proliferation in SW + MB0.225 group and SW + MB0.45 group, and obvious collagenous fiber proliferation in SW + MB0.9 group and SW + MB1.8 group (Figure 5A). The damage of nucleus, mitochondria, and sarcoplasmic reticulum in 6 groups were observed by TEM at 2 different magnification (2500 times and 7000 times). Normal myocardial cells can be seen in groups of N, SW, SW + MB0.225, and SW + MB0.45. Cytoplasmic swelling can be seen in SW + MB0.225 group. In SW + MB0.45 group, cytoplasmic swelling and slight mitochondrial swelling were observed. In SW + MB0.9 group, the cytoplasm swelled obviously, some cristae of mitochondria broke and disappeared with part of cristae fused. In SW + MB1.8 group, the cytoplasm and nucleus were swollen, the mitochondrial membrane was

A HE staining



B Masson's trichrome staining

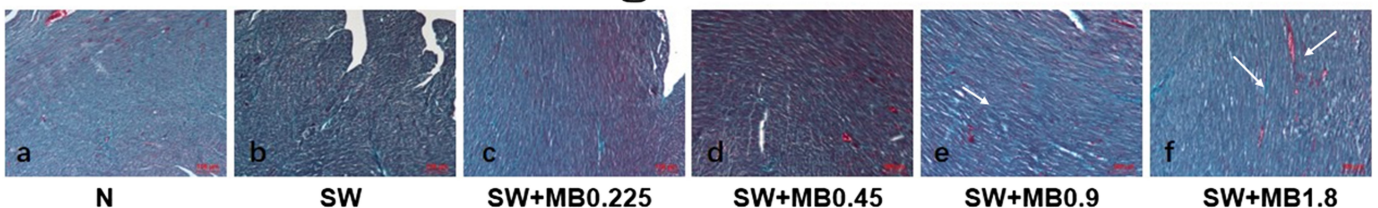
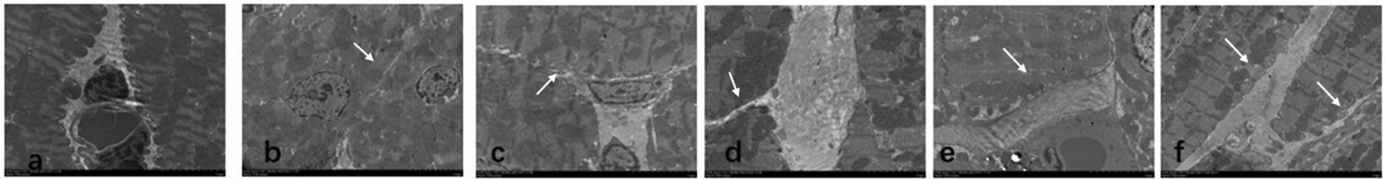
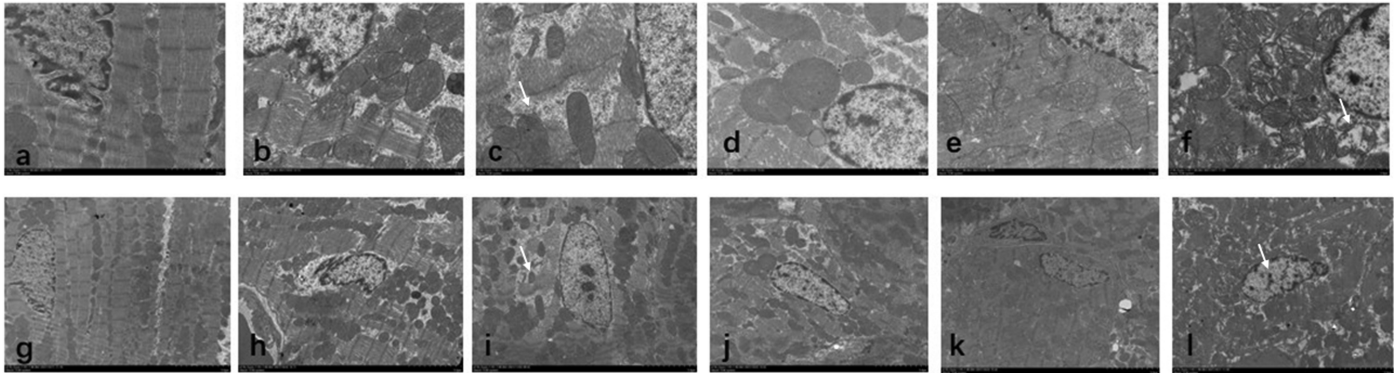


Figure 4. Histochemical methods were used to observe the morphological changes of rat heart tissue after extracorporeal shock wave combined with ultrasound microbubbles of different concentrations. (A) Hematoxylin eosin staining showed no inflammatory cell infiltration in group N (a), SW (b), SW + MB0.225 (c), SW + MB0.45 (d), and SW + MB0.9 (e). In SW + MB1.8 group (f), (→) shows inflammatory cell infiltration. **(B)** Masson staining showed no signs of fibrosis in N group (a), SW group (b), SW + MB0.225 group (c), SW + MB0.45 group (d), SW + MB0.9 group (e), and the heart, while SW + MB1.8 group (f) indicated fibrosis. Scale bar: 100 μm. MB, microbubble; SW, shock wave.

A. accumulation of collagen



B. myocardial ultrastructure



N

SW

SW+MB0.225

SW+MB0.45

SW+MB0.9

SW+MB1.8

Figure 5. Effect of extracorporeal shock wave combined with ultrasound microbubbles of different concentrations on myocardial ultrastructure in rats observed by transmission electron microscope. (A) The changes in collagenous fiber were observed by transmission electron microscope. No collagenous fiber was found in group N (a) and group SW (b). Slight proliferation of collagenous fiber was observed in SW + MB0.225 group (c) and SW + MB0.45 group (d). In SW + MB0.9 group (e) and SW + MB1.8 group (f), collagenous fiber was obviously proliferated. Magnification 3000 \times . (B) The changes in nucleus, mitochondria, and sarcoplasmic reticulum were observed with transmission electron microscope. Normal myocardial cells were visible in group N (a, g) and SW (b, h), and no obvious damage was found. Mitochondrial swelling (\longrightarrow) was occasionally seen in group SW + MB0.225 (c, i) and SW + 0.45 (d, j). Perinuclear space widened, mitochondrial crista fusion and sarcoplasmic reticulum expanded in group SW + MB0.9 (e, k). Cytoplasmic swelling, nuclear edge shift, and mitochondrial model swelling were visible in group SW + MB1.8 (f, l). Some mitochondrial crista breaks disappeared and sarcoplasmic reticulum expanded. a, b, c, d, e, f, Magnification 2500 \times ; g, h, i, j, k, l, Magnification 7000 \times . MB, microbubble; SW, shock wave.

partially broken, and the sarcoplasmic reticulum was partially collapsed (Figure 5B). Evaluate myocardial ultrastructure damage according to the myocardial ultrastructure damage scoring system proposed by Yildirim. There were significant differences among groups (chi-square = 26.99, $df = 5$, $P < .001$). The score of SW + MB1.8 group was significantly higher than that of the normal control group, SW group, SW + MB0.225 group, and SW + MB0.45 group ($P = .01$, $P = .02$, $P = .009$, $P = .028$). The score of SW + MB0.9 group was significantly higher than that of the normal control group ($P = .09$), and there was no significant difference between the rest groups.

Expression of Vascular Endothelial Growth Factor and eNOS Protein in Myocardium

Western blot results showed that the expressions of VEGF and eNOS protein in SW + MB0.225 group, SW + MB0.45 group, SW + MB0.9 group, and SW + MB1.8 group were higher than those in N group and SW group of which the strongest expression was in SW + MB0.45 group (Figure 6).

DISCUSSION

Extracorporeal SW therapy provides a new treatment option for patients with advanced CHD. The extracorporeal

cardiac SW system was developed by Swiss STORZ MEDICAL Company in 2003. Extracorporeal cardiac SW is a kind of low energy, narrow pulse width pulse mechanical wave. The waveform has a steep pulse rising section with a very short duration. It has very high pressure at the peak of the pulse. The focal pressure can reach 3~75 MPa, the frequency of the SW is 0.1~0.2 MHz, and the energy flow density is 0.005~0.640 mJ/mm², which is only 1/10 of the extracorporeal lithotripsy energy.¹⁶ The sulfur hexafluoride MB consists of a sulfur hexafluoride gas core and an external phospholipid shell, with a diameter of about 2.5 μ m.¹⁷ Sulfur hexafluoride MB can display 2 states in the application process, stable cavitation, and inertial cavitation. The research shows that the MB will produce inertial cavitation when the pressure is greater than 1.5 MPa, which will result in nonlinear increase of the MB volume and crack.¹⁸ The focal pressure of extracorporeal cardiac SW is about 3~75 MPa, which is enough to cause inertial cavitation of MBs. In vitro experiments, we found that the intensity of extracorporeal cardiac SW treatment can accelerate the destruction of ultrasound MBs and enhance cavitation. However, previous studies have shown that excessive cavitation also has harmful effects on normal cells and tissues, such as bleeding, vascular injury, apoptosis, etc.¹⁹⁻²² Therefore, it is necessary to conduct a more in-depth and

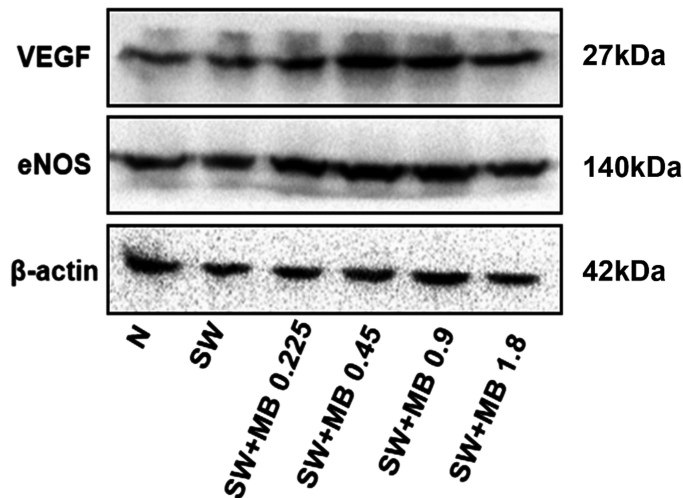


Figure 6. Expression of VEGF and eNOS protein in myocardium after extracorporeal shock wave combined with microbubbles of different concentrations. The expressions of VEGF and eNOS protein in SW+MB0.225 group, SW+MB0.45 group, SW+MB0.9 group, and SW+MB1.8 group were higher than that in the N group and SW group, and the strongest expression was in SW+MB0.45 group. MB, microbubble; SW, shock wave; VEGF, vascular endothelial growth factor.

comprehensive exploration of the combination and evaluate it in the clinical environment.

Extracorporeal cardiac SW therapy will not cause additional damage to the body. Studies reported that²³ after extracorporeal cardiac SW therapy, no hemodynamic abnormalities, arrhythmia, and cTnI elevation were observed in rats, and no adverse effects on left ventricular function were found by cardiac ultrasound evaluation. In our study, no arrhythmia was found in rats, and there was no difference in heart rate, blood pressure, LVIDs, EDV, ESV, EF, and FS before and after treatment compared with the control group, which was consistent with previous studies. However, the level of cTnI in serum increased significantly in SW+MB0.9 group and SW+MB1.8 group, which may be due to the increased concentration of MBs, the increased number of MBs in the myocardium, and the significant inertial cavitation, which led to myocardial cell damage. The immunohistochemical method was used to observe the myocardial tissue of rats after treatment. Neutrophils and lymphocytes were infiltrated in SW+MB0.9 group and SW+MB1.8 group. This may be due to infiltration and proliferation after external stimulation, which is also a reaction of the body's normal defense system. In addition, the degree of fibrosis in the SW+MB1.8 group increased. It is reported that²⁴ if the shearing stress and cavitation are strong enough during SW treatment, the cell membrane, cytoskeleton, small blood vessels, and other structures could be damaged and fibrosis could occur.

Previous studies have shown that²³ low energy SW induced in vitro is nonselective in treatment, generating mechanical shearing force and cavitation effect in tissues and cells further triggered a series of biochemical reactions at the

subcellular level. Based on the above factors, we used TEM to observe the myocardial ultrastructure. Transmission electron microscopy has 10 000 times magnification and nanometer resolution, which makes it have significant advantages in morphological evaluation at the cellular level. In 2004, Yildirim et al¹⁵ proposed a scoring system for myocardial ultrastructure damage in a series of studies. In this study, we mainly focus on the observation of the structure of nucleus, mitochondria, sarcoplasmic reticulum, and collagen fibers. According to the observed morphological changes, we scored 0~3. Liu et al²⁵ found that extracorporeal SW therapy did not cause significant damage to the ultrastructure of myocardial cells by the observation of the ultrastructure of myocardial cells with TEM, confirming that it was safe at the cellular level. Our research shows that the rats in SW group have normal myocardial cells, and mitochondria swelling can be seen occasionally in SW+MB0.225 group and SWB 0.45 group, which is consistent with previous research. However, in the SW+MB0.9 group, the perinuclear space widened, the mitochondrial crista fused, and the sarcoplasmic reticulum expanded. In the SW+MB1.8 group, the rat cardiac myocytes showed cytoplasmic swelling, nuclear edge shift, mitochondrial model swelling, partial crista rupture disappearance, and sarcoplasmic reticulum expansion. The myocardial injury score was significantly different from the control group. In addition, collagenous fiber was obviously proliferated in SW+MB0.9 group and SW+MB1.8 group, which indicated that with the increase of MB concentration, increased cavitation and shearing stress would damage the ultrastructure of the heart. The increase of collagenous fiber may be the result of self-repair after myocardial injury.

Previous studies have shown that^{26,27} the shearing stress and cavitation effect generated by extracorporeal cardiac SW and ultrasound MBs can significantly improve the levels of NO and VEGF. In this study, we have verified whether the combination of extracorporeal cardiac SW and ultrasound MBs with different concentrations can promote the cavitation effect. Nitric oxide has an important protective effect on the cardiovascular system since it regulates human vascular tension and causes endothelium-dependent vasodilation. Previous studies²⁸ showed that extracorporeal cardiac SW therapy can up-regulate the expression of VEGF and other cytokines and play a role in protecting ischemic myocardium by promoting the "budding" growth of capillaries, forming a new capillary network and inducing cardiac vasodilation.

In this study, we found that the serum NO level of rats treated with extracorporeal cardiac SW combined with ultrasound MBs of different concentrations was higher than that of rats treated with SW alone. Western blot results also showed that the expression levels of eNOS and VEGF in rats treated with different concentrations of sulfur hexafluoride MBs were higher than those treated with SW alone. We speculate the mechanism may be that the superimposed MB rupture in the myocardial microcirculation enhances the shear force and cavitation effect of extracorporeal cardiac SW, thereby enhancing the activity of endothelial NO synthase, promoting the production of NO, and can significantly up-regulate the expression of vascular endothelial growth

factor in ischemic myocardium, increase the capillary density of ischemic myocardium, and significantly increase the local blood perfusion in myocardial tissue. However, our study shows that with the increase of ultrasound MB concentration, its therapeutic effect does not increase linearly. In this study, there was no significant difference in serum NO levels among SW+MB0.45 group, SW+MB0.9 group, and SW+MB1.8 group. In Western blot results, eNOS and VEGF were the highest in SW+MB0.45 group, while protein expression levels in SW+MB1.8 group decreased. The possible reasons lie in the following: (1) With the increase of MB concentration, the ultrastructure of myocardial cells is damaged, which affects the normal function of myocardial cells and leads to the decrease of eNOS and VEGF levels in myocardial tissue; (2) when too many MBs are gathered together, the pressure generated by the explosion of the center MB will affect the surrounding MB, reducing its pressure instead. A high concentration of MBs may limit the growth of MBs, and blasting shearing stress may not produce the best clinical effect;²⁵ and (3) previous studies on sulfur hexafluoride MBs showed that^{29,30} the inertial cavitation threshold of MBs rises with the increase of bubble concentration. When the MB concentration is high, higher pressure is usually required to make the MB inertial cavitation. However, we did not adjust the focused pressure of extracorporeal SW with the increase of MB concentration during treatment.

In this study, we identify our novel hypothesis that a proper concentration of sulfur hexafluoride MBs could promote the cavitation effect of extracorporeal cardiac SWs. These findings indicated that combination therapy of extracorporeal cardiac SWs with sulfur hexafluoride MBs may become a new paradigm in CHD, especially contributing to the treatment of refractory angina. Especially, the new therapy paradigm provides a noninvasive approach for the assessment of myocardial structure and function in animal and clinical studies. More importantly, the combined-modality treatment may provide theoretical support for the treatment of patients with CHD, especially contributing to the treatment of refractory angina.

In this study, normal rats were selected and the observation time was relatively short. As well, our research has shortcomings in that female rats were not adopted to identify the cavitation effect of the combined-modality treatment. Thus, different outcomes might be found in the female model. Therefore, the safety and therapeutic effect in different heart disease models will be further observed in the follow-up study, and the long-term cardiac changes after treatment will also be evaluated. In addition, the patient had slight tingling during the clinical extracorporeal SW treatment. However, we cannot verify whether the combination of sulfur hexafluoride MBs will increase the pain due to the anesthesia of the animal.

CONCLUSION

In conclusion, the treatment of extracorporeal SW combined with sulfur hexafluoride MBs of different concentrations is feasible. The appropriate concentration of sulfur hexafluoride MBs does not cause damage to the myocardial

ultrastructure of rats, while myocardial ultrastructure will be injured when the concentration reaches 1.8 mL/kg/min. In addition, the combination of sulfur hexafluoride MBs could enhance the cavitation effect of extracorporeal cardiac SWs.

Ethics Committee Approval: The animal protocol of this study was approved by the Animal Ethics Committee of the Second Hospital of Hebei Medical University (Shijiazhuang), Animal Care and Use Committee (IACUC) (Animal Ethics No.: 2022 - AE207). During the study, the operation and animal care of the animals were in accordance with the Laboratory Animal Care and Use Guide.

Peer-review: Externally peer-reviewed.

Author Contributions: Concept – Y.M., X.W., H.Y., R.H.; Design – Y.M., X.W., H.Y., R.H.; Supervision – Y.M., X.W., H.Y., R.H.; Resources – Y.M., X.W., H.Y., R.H.; Materials – Y.M., X.W., H.Y., R.H.; Data Collection and/or Processing – Y.M., X.W., H.Y., R.H.; Analysis and/or Interpretation – Y.M., X.W., H.Y., R.H.; Literature Search – Y.M., X.W., H.Y., R.H.; Writing – Y.M., X.W., H.Y., R.H.; Critical Review – Y.M., X.W., H.Y., R.H.

Acknowledgment: We thank the transmission electron microscope research work of the Electron Microscope Center of Hebei Medical University, Meng Li for helping us make electron microscope samples, and Zhou Chenming for analyzing electron microscope images.

Declaration of Interests: The authors have no conflict of interest to declare.

Funding: The authors declared that this study has received no financial support.

REFERENCES

1. Compiling group of China cardiovascular Health and Disease Report. Essential introduction of China cardiovascular health and disease report 2020. *Chin J Cardiol.* 2021;26(3):209-218.
2. Blumenthal DM, Howard SE, Searl Como J, et al. Prevalence of angina among primary care patients with coronary artery disease. *JAMA Netw Open.* 2021;4(6):e2112800. [CrossRef]
3. Gallone G, Baldetti L, Tzanis G, et al. Refractory angina: from pathophysiology to new therapeutic nonpharmacological technologies. *JACC Cardiovasc Interv.* 2020;13(1):1-19. [CrossRef]
4. Yang HT, Xie X, Hou XG, Xiu WJ, Wu TT. Cardiac shock wave therapy for coronary heart disease: an updated meta-analysis. *Braz J Cardiovasc Surg.* 2020;35(5):741-756. [CrossRef]
5. Neri M, Riezzo I, Pascale N, Pomara C, Turillazzi E. Ischemia/reperfusion injury following acute myocardial infarction: A Critical Issue for Clinicians and Forensic Pathologists. *Mediators Inflamm.* 2017;2017:7018393. [CrossRef]
6. Weijing L, Ximin F, Jianying S, et al. Cardiac shock wave therapy ameliorates myocardial ischemia in patients with chronic refractory angina pectoris: A randomized trial. *Front Cardiovasc Med.* 2021;8:664433. [CrossRef]
7. Qiu Q, Shen T, Yu X, et al. Cardiac shock wave therapy alleviates hypoxia/reoxygenation-induced myocardial necroptosis by modulating autophagy. *BioMed Res Int.* 2021;2021:8880179. [CrossRef]
8. Zhang Y, Shen T, Liu B, et al. Cardiac shock wave therapy attenuates cardiomyocyte apoptosis after acute myocardial infarction in rats. *Cell Physiol Biochem.* 2018;49(5):1734-1746. [CrossRef]
9. Wang L, Tian X, Cao Y, et al. Cardiac shock wave therapy improves ventricular function by relieving fibrosis through PI3K/

- Akt signaling pathway: evidence from a rat model of post-infarction heart failure. *Front Cardiovasc Med*. 2021;8:693875. [\[CrossRef\]](#)
10. Chinese College of Cardiovascular Physicians, Cardiac Rehabilitation Management Committee of Chinese Hospital Association, Chinese Journal of Cardiovascular Medicine Editorial Committee. Chinese expert consensus on extracorporeal shock wave therapy for coronary heart disease (2022 version). *Chin J Cardiol*. 2022;27(1):1-10.
 11. Mott B, Ammi AY, Le DE, et al. Therapeutic ultrasound increases myocardial blood flow in ischemic myocardium and cardiac endothelial cells: results of in vivo and in vitro experiments. *J Am Soc Echocardiogr*. 2019;32(9):1151-1160. [\[CrossRef\]](#)
 12. Yu FTH, Chen X, Straub AC, Pacella JJ. The role of nitric oxide during Sonoreperfusion of microvascular obstruction. *Theragnostics*. 2017;7(14):3527-3538. [\[CrossRef\]](#)
 13. Park D, Song G, Jo Y, et al. Sonophoresis using ultrasound contrast agents: dependence on concentration. *PLOS ONE*. 2016;11(6):e0157707. [\[CrossRef\]](#)
 14. Su HL, Qian YQ, Wei ZR, et al. Real-time myocardial contrast echocardiography in rat: infusion versus bolus administration. *Ultrasound Med Biol*. 2009;35(5):748-755. [\[CrossRef\]](#)
 15. Yildirim E, Solaroglu I, Okutan O, et al. Ultrastructural changes in tracheobronchial epithelia following experimental traumatic brain injury in rats: protective effect of erythropoietin. *J Heart Lung Transplant*. 2004;23(12):1423-1429. [\[CrossRef\]](#)
 16. Wang M, Yang D, Hu Z, et al. Extracorporeal cardiac shock waves therapy improves the function of endothelial progenitor cells after hypoxia injury via activating PI3K/Akt/eNOS signal pathway. *Front Cardiovasc Med*. 2021;8:747497. [\[CrossRef\]](#)
 17. Schneider M, Arditi M, Barrau MB, et al. BR1: a new ultrasonographic contrast agent based on sulfur hexafluoride-filled microbubbles. *Invest Radiol*. 1995;30(8):451-457. [\[CrossRef\]](#)
 18. Lin Y, Lin L, Cheng M, et al. Effect of acoustic parameters on the cavitation behavior of SonoVue microbubbles induced by pulsed ultrasound. *Ultrason Sonochem*. 2017;35(A):176-184. [\[CrossRef\]](#)
 19. Aggeli C, Giannopoulos G, Lampropoulos K, Pitsavos C, Stefanadis C. Adverse bioeffects of ultrasound contrast agents used in echocardiography: true safety issue or "much ado about nothing". *Curr Vasc Pharmacol*. 2009;7(3):338-346. [\[CrossRef\]](#)
 20. Miller DL, Li P, Dou C, Gordon D, Edwards CA, Armstrong WF. Influence of contrast agent dose and ultrasound exposure on cardiomyocyte injury induced by myocardial contrast echocardiography in rats. *Radiology*. 2005;237(1):137-143. [\[CrossRef\]](#)
 21. Miller DL, Gies RA. The influence of ultrasound frequency and gas-body composition on the contrast agent-mediated enhancement of vascular bioeffects in mouse intestine. *Ultrasound Med Biol*. 2000;26(2):307-313. [\[CrossRef\]](#)
 22. Xie Y, Hu J, Lei W, Qian S. Prediction of vascular injury by cavitation microbubbles in a focused ultrasound field. *Ultrason Sonochem*. 2022;88:106103. [\[CrossRef\]](#)
 23. Di Meglio F, Nurzynska D, Castaldo C, et al. Cardiac shock wave therapy: assessment of safety and new insights into mechanisms of tissue regeneration. *J Cell Mol Med*. 2012;16(4):936-942. [\[CrossRef\]](#)
 24. Jargin SV. Shock wave therapy of ischemic heart disease in the light of general pathology. *Int J Cardiol*. 2010;144(1):116-117. [\[CrossRef\]](#)
 25. Liu B, Zhang Y, Jia N, et al. Study of the safety of extracorporeal cardiac shock wave therapy: observation of the ultrastructures in myocardial cells by transmission electron microscopy. *J Cardiovasc Pharmacol Ther*. 2018;23(1):79-88. [\[CrossRef\]](#)
 26. Burneikaitė G, Shkolnik E, Čelutkienė J, et al. Cardiac shock-wave therapy in the treatment of coronary artery disease: systematic review and meta-analysis. *Cardiovasc Ultrasound*. 2017;15(1):11. [\[CrossRef\]](#)
 27. Belcik JT, Mott BH, Xie A, et al. Augmentation of limb perfusion and reversal of tissue ischemia produced by ultrasound-mediated microbubble cavitation. *Circ Cardiovasc Imaging*. 2015;8(4). [\[CrossRef\]](#)
 28. Peng YZ, Zheng K, Yang P, et al. Shock wave treatment enhances endothelial proliferation via autocrine vascular endothelial growth factor. *Genet Mol Res*. 2015;14(4):19203-19210. [\[CrossRef\]](#)
 29. Chang PP, Chen WS, Mourad PD, Poliachik SL, Crum LA. Thresholds for inertial cavitation in albumin suspensions under pulsed ultrasound conditions. *IEEE Trans Ultrason Ferroelectr Freq Control*. 2001;48(1):161-170. [\[CrossRef\]](#)
 30. Yasui K, Lee J, Tuziuti T, Towata A, Kozuka T, Iida Y. Influence of the bubble-bubble interaction on destruction of encapsulated microbubbles under ultrasound. *J Acoust Soc Am*. 2009;126(3):973-982. [\[CrossRef\]](#)